




Half-integer quantized charge pumping induced by a Majorana fermionWei Luo ^{1,2,*} Weiyin Deng ³ and Ming-Xun Deng⁴¹*School of Science, Jiangxi University of Science and Technology, Ganzhou 341000, China*²*National Laboratory of Solid State Microstructures and Department of Physics, Nanjing University, Nanjing 210093, China*³*Department of Physics, South China University of Technology, Guangzhou 510640, China*⁴*Guangdong Provincial Key Laboratory of Quantum Engineering and Quantum Materials, ICMP and SPTE, South China Normal University, Guangzhou 510006, China* (Received 24 November 2020; revised 15 February 2021; accepted 1 March 2021; published 12 March 2021)

We investigate the adiabatic topological charge pumping in a topological superconductor utilizing a quantum anomalous Hall insulator proximity coupled to an s -wave superconductor. We show that topological pumping is characterized by the appearance of protected Majorana edge states during the course of a pumping cycle. In a topological superconductor with a single Majorana edge state, the Majorana state will be pushed into the electrode in a cycle. This leads to a half-integer quantized pumped charge, because a Majorana fermion can be viewed as half of a fermion. The half-integer quantized charge pumping would serve as a fingerprint of a Majorana fermion.

DOI: [10.1103/PhysRevB.103.125126](https://doi.org/10.1103/PhysRevB.103.125126)**I. INTRODUCTION**

Majorana fermions [1,2] have attracted extensive studies in recent years for they obey non-Abelian braiding statistics and have potential application in fault-tolerant quantum computations [1–9]. A Majorana fermion is an antiparticle of itself. Due to this self-Hermitian property, Majorana fermions lead to a number of interesting transport phenomena such as fractional Josephson effects [1,10,11], resonant Andreev reflections [12,13], and enhanced [14], and resonant [15] crossed Andreev reflections, as well as selective equal-spin Andreev reflections [15,16], which have potential application in spintronics.

In 2010, Qi *et al.* proposed that a quantum anomalous Hall insulator (QAHI) proximitized to an s -wave superconductor could realize a chiral topological superconductor (TSC) [17]. The QAHI with Chern number $\mathcal{C} = 1$ is topologically equivalent to a chiral TSC with Chern number $\mathcal{N} = 2$, when the induced superconducting pairing is infinitesimal. When the pairing potential increases, one of the two chiral Majorana edge modes in the $\mathcal{N} = 2$ chiral TSC is annihilated, and a new $\mathcal{N} = 1$ chiral TSC phase with a single chiral Majorana edge mode emerges. Later theoretical studies showed that the $\mathcal{N} = 1$ chiral TSC can give rise to a half-quantized longitudinal conductance plateau $e^2/2h$ in a QAHI-chiral TSC-QAHI junction [18,19], which was experimentally observed soon after [20].

The half-quantized longitudinal conductance plateau, and the zero bias conductance peak which comes from resonant Andreev reflection [12,13] and has been observed experimentally [21,22], are regarded as hallmarks of Majorana fermion. However, there is still a strong debate over the existence

of Majorana fermion, because both transport properties can possibly be attributed to trivial reasons. For example, Andreev bounded states [23], the Kondo effect [24], and weak antilocalization [25] may cause zero bias conductance peak, while the half-quantized conductance plateau may come from a metallic phase [26–29]. So other evidence to verify the existence of a Majorana fermion is desirable.

On the other hand, topological charge pump is a dynamic transport mechanism that dc current can flow in the absence of any applied bias voltage via a quantum system, in which two or more independent parameters are periodically modulated in time. It was originally proposed by Thouless and co-workers in the 1980s, who showed that the amount of charge pumped per cycle is directly related to a topological invariant of the system, namely, the Chern number [30], first introduced to classify the integer quantum Hall effect [31]. A Thouless pump may therefore be regarded as a dynamical version of the integer quantum Hall effect and enabled the direct measurement of the topological invariant of a bulk. The intriguing relation stimulates recent progresses in cold atomic systems, as exemplified by experimental realization of the quantized charge pump in atomic gases [32,33] following the theoretical proposal in the superlattice [34–36].

In this work, we investigate the quantum pumping in the chiral TSC. It is found that when an ac Zeeman field along the z direction, and an ac electric field along x direction, are applied, there appears a dc current in the y direction. We use the Chern number to describe the pump and find that there are three topological pumping regions, $\mathcal{N} = 0, 1, 2$. The pump with $\mathcal{N} = 0$ is trivial, and that with $\mathcal{N} = 2$ is topologically equivalent to a Chern pump which pumps an electron charge e into the electrode per cycle. At the transition between the two pumps, the new pump with $\mathcal{N} = 1$ gives an exotic half-integer quantized pumped charge $e/2$. We show that the half-integer quantized charge pumps are characterized by the appearance

*jxluow@163.com

of protected gapless Majorana edge states during the course of a pumping cycle, similar to the integer topological pump [37,38]. For a chiral TSC with $\mathcal{N} = 1$, when time changes a period, the Majorana edge state connecting the conduction and valence bands is pushed into the electrode. This leads to a half-integer quantized pumped charge $e/2$, because a Majorana fermion can be view as half of a regular fermion. The half-integer quantized charge pumping is directly related to the Majorana edge state and so can serve as a signature of a Majorana fermion. Our work is different from previous works about Majorana-mediated charge pumps [39–41], in which the pumped charge is not half-integer quantized, even not quantized, because they are not directly related to a topological invariant.

II. MODEL HAMILTONIAN

To start, we consider the superconductor proximity effect of the QAHI in a magnetic topological insulator thin film with ferromagnetic order. For definiteness, we adopt the simplest QAHI model Hamiltonian realized with low-energy states near the Γ point [17]:

$$H_{\text{QAHI}} = \begin{bmatrix} m_0 + Bk^2 & A(k_x - ik_y) \\ A(k_x + ik_y) & -m_0 - Bk^2 \end{bmatrix}, \quad (1)$$

where A is the spin-orbit coupling strength, and m_0 is the ferromagnetic exchange field. The basis vector is $(c_{\mathbf{k}\uparrow}, c_{\mathbf{k}\downarrow})^T$ with $c_{\mathbf{k}\sigma}$ annihilating an electron of momentum \mathbf{k} and $\sigma = \uparrow, \downarrow$. The sign of m_0/B determines the topological properties of the system, and the QAHI with $\mathcal{C} = 1$ is obtained when $m_0/B < 0$.

In proximity to an s -wave superconductor, a finite pairing potential Δ can be induced in QAHI. This gives us the Bogoliubov–de Gennes (BdG) Hamiltonian

$$H_{\text{BdG}} = \frac{1}{2} \begin{bmatrix} H_{\text{QAHI}}(\mathbf{k}) + \mu & i\Delta\sigma_y \\ -i\Delta^*\sigma_y & -H_{\text{QAHI}}^*(-\mathbf{k}) - \mu \end{bmatrix}, \quad (2)$$

where μ is chemical potential and the basis vector is $(c_{\mathbf{k}\uparrow}, c_{\mathbf{k}\downarrow}, c_{-\mathbf{k}\uparrow}^\dagger, c_{-\mathbf{k}\downarrow}^\dagger)^T$. When the pairing potential Δ increases from 0, the system could experience a series of topological phase transitions from $\mathcal{N} = 2$ to $\mathcal{N} = 1$ and then to $\mathcal{N} = 0$ with \mathcal{N} being the Chern number. The $\mathcal{N} = 2$ and $\mathcal{N} = 0$ phases are respectively topological equivalent to a QAHI with $\mathcal{C} = 1$ and trivial insulator with $\mathcal{C} = 0$, and the $\mathcal{N} = 1$ phase is a new TSC which hosts a chiral Majorana fermion mode at its edge.

To derive the quantum pumping, at least two time-dependent fields need to be imposed on the system. Here we applied a time-dependent Zeeman field along the z direction of the form $B_z(t) = m_1 \cos(\omega t)$, and an ac electric field along the x direction, $E_x(t) = E_x \cos(\omega t)$. The Zeeman field can enter into the Hamiltonian through replacing m_0 with $m(t) = m_0 + m_1 \cos(\omega t)$, and the electric field enters into the Hamiltonian through Peierls substitution $k_x \rightarrow \tilde{k}_x = k_x - eA_x(t)$, with e the electron charge and $A_x(t)$ the vector potential satisfying $E_x = -\partial A_x(t)/\partial t$. Now the diagonal components in Hamiltonian (2) is rewritten as

$$H_{\text{p}} = \begin{bmatrix} m(t) & A(\tilde{k}_x - ik_y) \\ A(\tilde{k}_x + ik_y) & -m(t) \end{bmatrix}. \quad (3)$$

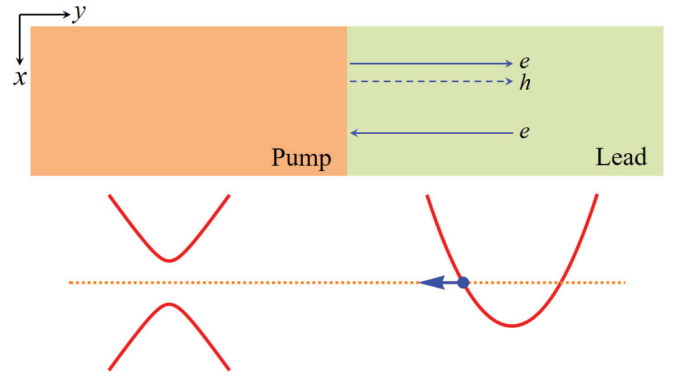


FIG. 1. Illustration of a pump/normal-metal junction and its energy band. The transport is along the y direction, and the transverse width of the pump is L_x .

Here we have set $\mu = 0$ and neglected the quadratic term for simplicity. Within the adiabatic approximation, it is easy to obtain for the eigenenergies of the pump at any given time t

$$E(\tilde{\mathbf{k}}) = \pm \sqrt{[m(t) \pm \Delta]^2 + A^2(\tilde{k}_x^2 + k_y^2)}. \quad (4)$$

One can see that if $|m_1| \geq |m_0 \pm \Delta|$, at $\cos \omega t = \frac{m_0 \pm \Delta}{m_1}$, the conduction and valence bands touch at $k_y = 0$, and $k_x^c = k_{x\pm}^c$ or $-k_{x\pm}^c$, with $k_{x\pm}^c = |eA_x \frac{\sqrt{m_1^2 - (m_0 \pm \Delta)^2}}{m_1}|$.

III. CHARGE PUMPING FROM THE SCATTERING MATRIX FORMULA

The amount of charge pumped per cycle can be conveniently calculated by using the scattering matrix formula [42,43]. We consider the pump placed in $y < 0$ is linked to an electrode for $y > 0$, and they are in good contact with each other, as illustrated in Fig. 1. The Hamiltonian of pump is given by Eq. (2) with diagonal component replaced by Eq. (3). The electrode is taken to be a normal metal with a 2D parabolic Hamiltonian $H_E = -E_0 + p^2/2m$. When E_0 is sufficiently large, for a given p_x , we can linearize the effective 1D Hamiltonian H_E at the right and left Fermi points $p_y = \pm mv'_F(k_x)$ with $v'_F(k_x) = \sqrt{2m(E_F + E_0) - k_x^2}/m$. A Pauli matrix $\hat{\sigma}_y$ is introduced to describe the two branches. To be consistent with the form of the Hamiltonian (3) in the pump, we use $\sigma_y = 1$ and -1 , respectively, to represent the right-moving and left-moving branch. As a result, the Hamiltonian of the electrode becomes $H_E = v'_F(k_x)k_y\hat{\tau}_z\hat{\sigma}_y$ at $E_F = 0$, where $k_x = p_x$, $k_y = p_y \mp mv'_F(k_x)$, and $\hat{\tau}_z$ is a Pauli matrix acting on the Nambu space. When E_0 is sufficiently large, we can further approximate $v'_F(k_x) \approx v'_F(k_x = 0) = v'_F$, with the purpose of minimizing the number of adjustable parameters in the model.

Calculation of the charge pumped into the electrode per cycle amounts to solving the scattering problem of an incident at the Fermi level from the electrode. The Fermi energy is taken to be $E_F = 0$, which is in the band gap of the pump. In this case, the incident electron will be fully reflected back into the electrode as an electron or as a hole, which is called

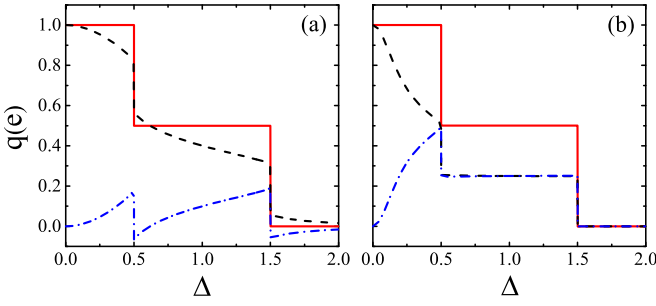


FIG. 2. Plot of charge pumped per cycle as a function of the pairing potential Δ . We have taken the units $m_1 = 1$ and $A = 1$, and set $m_0 = 0.5$, $eA_x = 0.1$, $k_x = 0$. The red solid line represents the total charge pumped; the black dashed line and blue dot-dashed line are the contributions of the normal reflection and Andreev reflection, respectively. Panel (a) is the result in the absence of quadratic term, and (b) contains the correction of the quadratic term.

Andreev reflection. The wave function in the lead is given by

$$\Psi_E(y) = \frac{1}{\sqrt{2}} \begin{pmatrix} 1 \\ -i \\ 0 \\ 0 \end{pmatrix} + \frac{r_{ee}}{\sqrt{2}} \begin{pmatrix} i \\ 0 \\ 0 \\ 0 \end{pmatrix} + \frac{r_{he}}{\sqrt{2}} \begin{pmatrix} 0 \\ 0 \\ 1 \\ -i \end{pmatrix}, \quad (5)$$

and that in the pump is

$$\Psi_P(y) = c_1 \begin{pmatrix} \sin \frac{\theta_1}{2} \\ \cos \frac{\theta_1}{2} \\ \cos \frac{\theta_1}{2} \\ \sin \frac{\theta_1}{2} \end{pmatrix} e^{\gamma_1 y} + c_2 \begin{pmatrix} \sin \frac{\theta_2}{2} \\ \cos \frac{\theta_2}{2} \\ -\cos \frac{\theta_2}{2} \\ -\sin \frac{\theta_2}{2} \end{pmatrix} e^{\gamma_2 y}, \quad (6)$$

where $\gamma_{1,2} = \sqrt{\tilde{k}_x^2 + \frac{[m(t) \pm \Delta]^2}{A^2}}$ and $\sin \theta_{1,2} = \frac{m(t) \pm \Delta}{A\gamma_{1,2}}$. We omit the plane wave factors $e^{ik_y y}$ in Eq. (5), because when the incident energy is $E_F = 0$, $k_y = 0$ and $e^{ik_y y} = 1$. Matching the wave functions (5) and (6) at $y = 0$ by using the boundary condition $\Psi_E(0^+) = \Psi_P(0^-)$, we can obtain the normal reflection r_{ee} and the Andreev reflection r_{he} as

$$\begin{aligned} r_{ee} &= -\frac{e^{i\theta_1} + e^{i\theta_2}}{2}, \\ r_{he} &= -i \frac{e^{i\theta_1} - e^{i\theta_2}}{2}. \end{aligned} \quad (7)$$

The charge pumped per cycle is given by [42,43]

$$q = \frac{e}{2\pi i} \oint_T \left(r_{ee}^* \frac{dr_{ee}}{dt} + r_{he}^* \frac{dr_{he}}{dt} \right), \quad (8)$$

with $T = 2\pi/\omega$ as a period of the pump. The first and second terms are the contributions of normal reflection and Andreev reflection, respectively. In Fig. 2(a) we show the pumped charge as a function of the pairing potential. One can see that when $\Delta = 0$, the system returns to the QAH and the contribution from Andreev reflection is vanishing [see Eq. (11)], so the pumped charge fully comes from the contribution of normal reflection, which gives the same result as the Chern pump $q = e$. When Δ increases from 0, the contribution from Andreev reflection increases and that of normal reflection decreases, while the total pumped charge keeps $q = e$ as long as

$\Delta < 0.5$. When the pairing potential exceeds 0.5, the charge pumped per cycle drops to half electron charge $q = e/2$. The half-integer quantized charge pumping will hold until the pairing potential exceeds 1.5. Last, when $\Delta > 1.5$, the contributions from normal reflection and Andreev reflection always cancel each other, giving rise to $q = 0$.

IV. THE TOPOLOGICAL ORIGIN OF HALF-INTEGER QUANTIZED PUMPED CHARGE

The above results that the charge pumped per cycle is always half-integer or integer quantized strongly suggest that the pumping effect in the chiral TSC has a topological origin. Now we will show that the half-integer quantized charge pumping is induced by a Majorana fermion. We first rewrite the BdG Hamiltonian into a block diagonal form using a new basis $\frac{1}{\sqrt{2}}(c_{\mathbf{k}\uparrow} + c_{-\mathbf{k}\downarrow}^\dagger, c_{\mathbf{k}\downarrow} + c_{-\mathbf{k}\uparrow}^\dagger, -c_{\mathbf{k}\uparrow} + c_{-\mathbf{k}\downarrow}^\dagger, -c_{\mathbf{k}\downarrow} + c_{-\mathbf{k}\uparrow}^\dagger)$,

$$H_{\text{BdG}} = \begin{bmatrix} h_+(\mathbf{k}) & 0 \\ 0 & -h_-^*(-\mathbf{k}) \end{bmatrix},$$

with

$$h_\pm(\mathbf{k}) = \begin{bmatrix} m(t) \pm |\Delta| & A(\tilde{k}_x - ik_y) \\ A(\tilde{k}_x + ik_y) & -m(t) \mp |\Delta| \end{bmatrix}. \quad (9)$$

In this basis, one can conveniently obtain the Chern number, which is divided into two parts, namely, the Chern numbers \mathcal{N}_+ of $h_+(\mathbf{k})$ and \mathcal{N}_- of $-h_-^*(-\mathbf{k})$. \mathcal{N}_\pm are given by $\mathcal{N}_\pm = \frac{1}{\pi} \int_0^T dt \int_{-\infty}^{\infty} dk_y \text{Im} \langle \partial_t \psi_\pm | \partial_{k_y} \psi_\pm \rangle$, with $|\psi_\pm\rangle$ the occupied bands of $h_+(\mathbf{k})$ and $-h_-^*(-\mathbf{k})$. Through straightforward calculations, one can get the Chern numbers of the ground bands as

$$\mathcal{N}_\pm = \text{sgn}(m_1 A_x) \theta(|m_1| - |m_0 \pm \Delta|) \theta(k_{x\pm}^c - |k_x|). \quad (10)$$

Not surprisingly, the critical points are the band touching points.

The total Chern number of the system is $\mathcal{N} = \mathcal{N}_+ + \mathcal{N}_-$, which gives the number of edge states. Due to the self-Hermitian property of the new basis, for example, assuming that $\gamma_{\mathbf{k}\uparrow} = c_{\mathbf{k}\uparrow} + c_{-\mathbf{k}\downarrow}^\dagger$, it is easy to see that $\gamma_{\mathbf{k}\uparrow}^\dagger = \gamma_{-\mathbf{k}\downarrow}$, the edge states are Majorana fermions. To see the Majorana edge states, we consider the spectrum of the instantaneous energies on an open chain of 40 sites. The equivalent tight-binding Hamiltonian of the open chain is given by

$$\begin{aligned} H' &= \sum_{\langle ij \rangle} c_i^\dagger (t_0 \hat{\sigma}_z + i t_1^{i,j} \hat{\sigma}_y) c_j + \sum_i m(t) c_i^\dagger \hat{\sigma}_z c_i \\ &+ \sum_i A \tilde{k}_x c_i^\dagger \hat{\sigma}_y c_i + \left(\sum_i \Delta c_i^\dagger c_{i\downarrow}^\dagger + \text{H.c.} \right), \end{aligned} \quad (11)$$

where $c_i^\dagger = (c_{i\uparrow}^\dagger, c_{i\downarrow}^\dagger)$ is the electron creation operator on site i , the angular bracket in $\langle i, j \rangle$ stands for nearest-neighboring sites, $t_0 = B/2$, and $t_1^{i,i+1} = -t_1^{i+1,i} = A/2$. In Fig. 3(a) we show the case of $\Delta = 0.3$, corresponding to the $q = e$ region in Fig. 2, for which $\mathcal{N} = 2$ with both $\mathcal{N}_\pm = 1$. One can easily distinguish the edge states from the bulk states. At a given Fermi energy, labeled by horizontal dashed line, there exist four edge states in the band gap. Through the analysis of the spatial distribution of the wave functions, as shown in

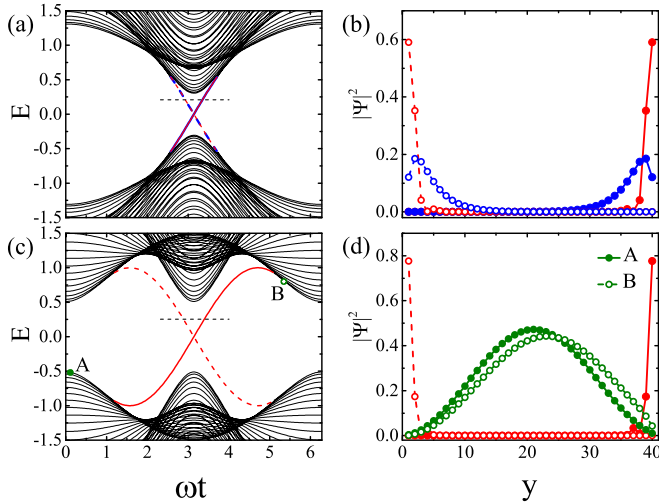


FIG. 3. Instantaneous spectrum of H_{BdG} versus time t in a ribbon for (a) $\Delta = 0.3$ and (c) $\Delta = 1$. The other parameters are the same as in Fig. 2. Panels (b) and (d) show the real-space probability distribution of the edge states corresponding to (a) and (c), respectively. The green lines in (d) represent the probability distribution of A and B in (c), which was magnified 10 times.

From Fig. 3(b), one can see that the two edge states represented by solid lines localize near one boundary, while the other two represented by dashed lines localize near the other boundary. When the pairing potential $\Delta = 1$, lying in the region of $q = e/2$, we have $\mathcal{N}_+ = 0$, $\mathcal{N}_- = 1$, and so there is only one chiral Majorana state localizing at each edge [see Fig. 3(c)], and corresponding density distribution is shown by the red lines in Fig. 3(d).

Different from the QAHI case, the Chern number \mathcal{N} in chiral TSC does not correspond to a quantized Hall conductance because charge is not conserved, while it also gives a physical observable, charge pumped, which is directly related to the edge states. We first consider the case of $\mathcal{N} = 1$. At $t = 0$, all the occupied valence bands are predominantly in the bulk; see the green point A in Figs. 3(c) and 3(d). As time increases, one state is pushed into the right edge region, with energy raised deep in the bulk band gap; see the red solid line in Figs. 3(c) and 3(d). Eigenstates cannot pile up in the right state region, so the state pumped to the right edge has to go somewhere. If the pump body is isolated, the only direction the Majorana edge state can go is back towards the bulk, acquiring enough energy to be in the upper band, as the green cycle B shown in Figs. 3(c) and 3(d). While when the pump is linked to an electrode, the case is different, the Majorana mode could continue to propagate to the right and enter into the electrode. Because the Majorana fermion can be viewed as half an electron, there is half electron charge $e/2$ pumped into the electrode. When $\mathcal{N} = 2$, there are two Majorana edge states pushed into the electrode per cycle, giving pumped charge $q = e$.

In the above discussion, we have shown that the half-integer quantized pumped charge in chiral TSC is induced by a Majorana fermion and described by the Chern number. Now we check the consistence of the scattering matrix formula and the topological description. In Fig. 4 we plot the charge pumped as a function of Δ and k_x . One can see that

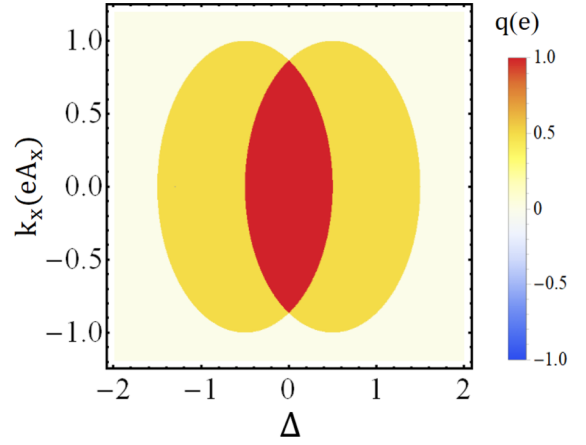


FIG. 4. Charge pumped versus Δ and k_x . The other parameters are the same as in Fig. 2.

the charge pumped per cycle is always half-integer or integer quantized, and consistent with the Chern number. The boundaries distinguishing different charge pumped are determined by $|k_x| = k_{x\pm}^c$, namely, the second θ function in Eq. (10).

By summing over k_x between $-k_{x\pm}^c$ and $k_{x\pm}^c$, we obtain for total charge pumped per cycle

$$q_t = \frac{eL_x}{2\pi} \sum_{\pm} \theta(|m_1| - |m_0 \pm \Delta|) k_{x\pm}^c, \quad (12)$$

with L_x the size of the pump along the x direction. When $\Delta = 0$, the pump returns to the general Chern pump, which is nontrivial when $|m_0| < |m_1|$, and trivial for $|m_0| > |m_1|$. So when m_1 is tuned to in the region $|m_0 + \Delta| < |m_1| < |m_0|$ or $|m_0 - \Delta| < |m_1| < |m_0|$, one can easily distinguish the pump induced by the Majorana fermion, which gives charge pumped $e/2$ for each $|k_x| < k_{x\pm}^c$ and total charge $\frac{eL_x k_{x\pm}^c}{2\pi}$, from the Chern pump giving charge pumped $q_t = 0$.

V. DISCUSSION AND SUMMARY

In the calculation, we neglect the quadratic term for simplicity. Now we emphasize that the quadratic term have no effect on the pumping. First, from the view of topology, when the quadratic term is included, one can easily see that the Chern number is Eq. (10) as well. It is noted that for the topological pumping effect, the Chern number is calculated on the torus of variables k_y and t . This is different from the case of QAHI, in which the Chern number is defined on the torus of k_x and k_y . Next, we further check our results from the scattering matrix formula. The electrode is also taken to be a QAHI, and the Hamiltonian is given by $H_E = -E_0 + H_{\text{QAHI}}$. When the incident energy is $E_F = 0$, one can obtain that the wave functions in the electrode and pump are $\Psi_E(y) = (\chi_+(-k_y^1), r_{he}^1 \chi_-(-k_y^1))^T e^{-ik_y^1 y} + (r_{ee}^1 \chi_+(k_y^1), \mathbf{0})^T e^{ik_y^1 y} + (r_{he}^2 \chi_+(k_y^2), r_{ee}^2 \chi_-(k_y^2))^T e^{ik_y^2 y}$, and $\Psi_P(y) = \sum_{i=1}^4 s_i (1, b(k_i), c(k_i), d(k_i))^T e^{ik_i y}$, where $\chi_{\pm}(k_y) = \frac{1}{N(k_y)} (A(k_x \mp ik_y), \mp(m_0 + Bk^2 - E_0))$ with $N(k_y)$ the normalization factor, $b(k_i) = \frac{2A(\tilde{k}_x + ik_i)m(t) + B\tilde{k}^2}{[m(t) + B\tilde{k}^2]^2 - A^2\tilde{k}^2 - \Delta^2}$, $c(k_i) = \frac{A(\tilde{k}_x + ik_i) - [m(t) + B\tilde{k}^2]b(k_i)}{\Delta}$, $d(k_i) = -\frac{[m(t) + B\tilde{k}^2] + A(\tilde{k}_x - ik_i)b(k_i)}{\Delta}$, wave

vectors $k_y^1 = \sqrt{[-\delta + \sqrt{\delta^2 + 4B^2(E_0^2 - m_0^2)}]/2B^2 - k_x^2}$, $k_y^2 = i\sqrt{[\delta + \sqrt{\delta^2 + 4B^2(E_0^2 - m_0^2)}]/2B^2 + k_x^2}$ with $\delta = 2m_0B + A^2$, and k_i are the four roots of the eigenequation $|H_{\text{BDG}}| = 0$ with negative imaginary parts. One can obtain the reflection coefficients by the boundary conditions and then charge pumped per cycle via Eq. (8). It is noted that the transport is fully determined by reflection amplitudes r_{ee}^1 and r_{he}^1 , while r_{ee}^2 and r_{he}^2 have no contributions because they are evanescent modes. The result is shown in Fig. 2(b), in which the total charge pumped per cycle is consistent with Fig. 2(a).

In summary, we have investigated the topological pumping effect in chiral TSC, modulated by a time-dependent Zeeman field and an ac electric field. We find that one, half one, or zero electron charge could be pumped from the pump body into the

electrode, depending on the strength of pairing potential Δ , ferromagnetic exchange field m_0 , and ac Zeeman field m_1 . We also show that the pumping is induced by Majorana fermion. When time-dependent fields change a period, if one Majorana state is pushed into the electrode, there will be half one electric charge pumped into the electrode because a Majorana fermion can be viewed as half of a fermion. The half-integer quantized charge pumping could serve as a fingerprint of a Majorana fermion.

ACKNOWLEDGMENTS

This work was supported by the National Natural Science Foundation of China under Grants No. 11804130 (W.L.), No. 11804101 (W.Y.D.), and No. 11904107 (M.X.D.) and the Jiangxi provincial Department of Science and Technology under Grant No. 20181BAB211008 (W.L.).

-
- [1] A. Y. Kitaev, *Phys. Usp.* **44**, 131 (2001).
 [2] F. Wilczek, *Nat. Phys.* **5**, 614 (2009).
 [3] M. Z. Hasan and C. L. Kane, *Rev. Mod. Phys.* **82**, 3045 (2010).
 [4] X. L. Qi and S. C. Zhang, *Rev. Mod. Phys.* **83**, 1057 (2011).
 [5] J. Alicea, *Rep. Prog. Phys.* **75**, 076501 (2012).
 [6] S. R. Elliott and M. Franz, *Rev. Mod. Phys.* **87**, 137 (2015).
 [7] C. W. J. Beenakker, *Annu. Rev. Condens. Matter Phys.* **4**, 113 (2013).
 [8] D. A. Ivanov, *Phys. Rev. Lett.* **86**, 268 (2001).
 [9] J. Alicea, Y. Oreg, G. Refael, F. von Oppen, and M. P. A. Fisher, *Nat. Phys.* **7**, 412 (2011).
 [10] H. J. Kwon, K. Sengupta, and V. M. Yakovenko, *Eur. Phys. J. B* **37**, 349 (2004).
 [11] L. Fu and C. L. Kane, *Phys. Rev. B* **79**, 161408(R) (2009).
 [12] K. T. Law, P. A. Lee, and T. K. Ng, *Phys. Rev. Lett.* **103**, 237001 (2009).
 [13] M. Wimmer, A. R. Akhmerov, J. P. Dahlhaus, and C. W. J. Beenakker, *New J. Phys.* **13**, 053016 (2011).
 [14] J. Nilsson, A. R. Akhmerov, and C. W. J. Beenakker, *Phys. Rev. Lett.* **101**, 120403 (2008).
 [15] J. J. He, J. Wu, T.-P. Choy, X.-J. Liu, Y. Tanaka, and K. T. Law, *Nat. Commun.* **5**, 3232 (2014).
 [16] J. J. He, T. K. Ng, P. A. Lee, and K. T. Law, *Phys. Rev. Lett.* **112**, 037001 (2014).
 [17] X. L. Qi, T. L. Hughes, and S. C. Zhang, *Phys. Rev. B* **82**, 184516 (2010).
 [18] S. B. Chung, X. L. Qi, J. Maciejko, and S. C. Zhang, *Phys. Rev. B* **83**, 100512(R) (2011).
 [19] J. Wang, Q. Zhou, B. Lian, and S. C. Zhang, *Phys. Rev. B* **92**, 064520 (2015).
 [20] Q. L. He, L. Pan, A. L. Stern, E. Burks, X. Che, G. Yin, J. Wang, B. Lian, Q. Zhou, E. S. Choi *et al.*, *Science* **357**, 294 (2017).
 [21] H. Zhang, C.-X. Liu, S. Gazibegovic, D. Xu, J. A. Logan, G. Wang, N. van Loo, J. D. S. Bommer, M. W. A. de Moor, D. Car *et al.*, *Nature (London)* **556**, 74 (2018).
 [22] D. Wang, L. Kong, P. Fan, H. Chen, S. Zhu, W. Liu, L. Cao, Y. Sun, S. Du, J. Schneeloch *et al.*, *Science* **362**, 333 (2018).
 [23] J. Liu, A. C. Potter, K. T. Law, and P. A. Lee, *Phys. Rev. Lett.* **109**, 267002 (2012).
 [24] E. J. H. Lee, X. Jiang, R. Aguado, G. Katsaros, C. M. Lieber, and S. De Franceschi, *Phys. Rev. Lett.* **109**, 186802 (2012).
 [25] D. I. Pikulin, J. P. Dahlhaus, M. Wimmer, H. Schomerus, and C. W. J. Beenakker, *New J. Phys.* **14**, 125011 (2012).
 [26] C.-Z. Chen, J. J. He, D.-H. Xu, and K. T. Law, *Phys. Rev. B* **96**, 041118(R) (2017).
 [27] W. Ji and X.-G. Wen, *Phys. Rev. Lett.* **120**, 107002 (2018).
 [28] Y. Huang, F. Setiawan, and J. D. Sau, *Phys. Rev. B* **97**, 100501(R) (2018).
 [29] B. Lian, J. Wang, X.-Q. Sun, A. Vaezi, and S.-C. Zhang, *Phys. Rev. B* **97**, 125408 (2018).
 [30] D. J. Thouless, *Phys. Rev. B* **27**, 6083 (1983).
 [31] D. J. Thouless, M. Kohmoto, M. P. Nightingale, and M. denNijs, *Phys. Rev. Lett.* **49**, 405 (1982).
 [32] S. Nakajima, T. Tomita, S. Taie, T. Ichinose, H. Ozawa, L. Wang, M. Troyer, and Y. Takahashi, *Nat. Phys.* **12**, 296 (2016).
 [33] M. Lohse, C. Schweizer, O. Zilberberg, M. Aidelsburger, and I. Bloch, *Nat. Phys.* **12**, 350 (2016).
 [34] L. Wang, M. Troyer, and X. Dai, *Phys. Rev. Lett.* **111**, 026802 (2013).
 [35] F. Mei, J.-B. You, D.-W. Zhang, X. C. Yang, R. Fazio, S.-L. Zhu, and L. C. Kwek, *Phys. Rev. A* **90**, 063638 (2014).
 [36] Y. Hatsugai and T. Fukui, *Phys. Rev. B* **94**, 041102(R) (2016).
 [37] D. Meidan, T. Micklitz, and P. W. Brouwer, *Phys. Rev. B* **82**, 161303(R) (2010).
 [38] D. Meidan, T. Micklitz, and P. W. Brouwer, *Phys. Rev. B* **84**, 195410 (2011).
 [39] M. Gibertini, R. Fazio, M. Polini, and F. Taddei, *Phys. Rev. B* **88**, 140508(R) (2013).
 [40] M. Alos-Palop, R. P. Tiwari, and M. Blaauboer, *Phys. Rev. B* **89**, 045307 (2014).
 [41] K. M. Tripathi, S. Rao, and S. Das, *Phys. Rev. B* **99**, 085435 (2019).
 [42] M. Büttiker, H. Thomas, and A. Prêtre, *Z. Phys. B* **94**, 133 (1994).
 [43] P. W. Brouwer, *Phys. Rev. B* **58**, R10135 (1998).